Received: 25 March 2023 | Revised: 30 September 2023 | Accepted: 6 October 2023

DOI: 10.1111/jnc.15996

Journal of Neurochemistry JNC The Official Journal of the International Society for Neurochemistry WILEY

ORIGINAL ARTICLE

Non-invasive in vivo measurements of metabolic alterations in the type 2 diabetic brain by ^{1}H magnetic resonance spectroscopy

In-Young Choi[1,2,3] | Wen-Tung Wang[1] | Bhumsoo Kim[4,5] | Junguk Hur[6] | David C. Robbins[7] | Dae-Gyu Jang[4,5] | Masha G. Savelieff[6] | Eva L. Feldman[4,5] | Phil Lee[1,3]

[1]Hoglund Biomedical Imaging Center, University of Kansas Medical Center (KUMC), Kansas City, Kansas, USA

[2]Department of Neurology, KUMC, Kansas City, Kansas, USA

[3]Department of Radiology, KUMC, Kansas City, Kansas, USA

[4]Department of Neurology, University of Michigan, Ann Arbor, Michigan, USA

[5]NeuroNetwork for Emerging Therapies, University of Michigan, Ann Arbor, Michigan, USA

[6]Department of Biomedical Sciences, University of North Dakota, Grand Forks, North Dakota, USA

[7]Department of Medicine, KUMC, Kansas City, Kansas, USA

Correspondence
In-Young Choi, University of Kansas Medical Center, Hoglund Biomedical Imaging Center, 3901 Rainbow Boulevard, Mailstop 1052, Kansas City, Kansas 66160, USA.
Email: ichoi@kumc.edu

Funding information
National Institutes of Health, Grant/Award Number: R21DK081079, M01RR023940, R01DK107956, R01DK129320 and R01DK130913; Andrea and Lawrence A. Wolfe Brain Health Initiative; Juvenile Diabetes Research Foundation United Kingdom, Grant/Award Number: 5COE-2019-861-S-B; Nathan and Rose Milstein Research Fund; NeuroNetwork for Emerging Therapies; Robert and Katherine Jacobs Environmental Health Initiative; Robert E. Nederlander Sr. Program for Alzheimer's Research; Sinai Medical Staff Foundation Research on Studying Diet and Brain Health

Abstract

Type 2 diabetes (T2D) is a complex chronic metabolic disorder characterized by hyperglycemia because of insulin resistance. Diabetes with chronic hyperglycemia may alter brain metabolism, including brain glucose and neurotransmitter levels; however, detailed, longitudinal studies of metabolic alterations in T2D are lacking. To shed insight, here, we characterized the consequences of poorly controlled hyperglycemia on neurochemical profiles that reflect metabolic alterations of the brain in both humans and animal models of T2D. Using in vivo ^{1}H magnetic resonance spectroscopy, we quantified 12 metabolites cross-sectionally in T2D patients and 20 metabolites longitudinally in T2D *db/db* mice versus *db+* controls. We found significantly elevated brain glucose (91%, $p<0.001$), taurine (22%, $p=0.02$), glucose+taurine (56%, $p<0.001$), *myo*-inositol (12%, $p=0.02$), and choline-containing compounds (10%, $p=0.01$) in T2D patients versus age- and sex-matched controls, findings consistent with measures in T2D *db/db* versus control *db+* littermates. In mice, hippocampal and striatal neurochemical alterations in brain glucose, ascorbate, creatine, phosphocreatine, γ-aminobutyric acid, glutamate, glutamine, glutathione, glycerophosphorylcholine, lactate, *myo*-inositol, and taurine persisted in *db/db* mice with chronic disease progression from 16 to 48 weeks of age, which were distinct from control *db+* mice. Overall, our study demonstrates the utility of ^{1}H magnetic resonance spectroscopy as a non-invasive tool for characterizing and monitoring brain metabolic changes with T2D progression.

KEYWORDS
brain metabolism, human brain, magnetic resonance spectroscopy, mouse, neurochemical profile, type 2 diabetes

Abbreviations: CSI, chemical shift imaging; GABA, γ-aminobutyric acid; MR, magnetic resonance; MRI, MR imaging; MRS, MR spectroscopy; NAA, N-acetylaspartate; NAAG, N-acetylaspartylglutamate; RF, radiofrequency; ROI, region of interest; T2D, type 2 diabetes; TE, echo time; TR, repetition time; VOI, volume of interest.

This article is part of the special issue "14th International Conference on Brain Energy Metabolism: Energy Substrates and Microbiome Govern Brain Bioenergetics and Cognitive Function with Aging".

 © 2023 International Society for Neurochemistry.

1 | INTRODUCTION

Type 2 diabetes (T2D) is a chronic metabolic disorder characterized by hyperglycemia because of insulin resistance (Ahmad et al., 2022). T2D prevalence continues to rise globally and currently affects around 540 million individuals (Sun et al., 2022). In addition to the challenges of controlling hyperglycemia, T2D patients are susceptible to a suite of diabetic complications, including damage to peripheral nerves (Elafros et al., 2022), eyes (Sabanayagam et al., 2019), kidneys (Thomas et al., 2015), and the cardiovascular system (Yun & Ko, 2021). Increasingly, structural changes to the brain in T2D are also reported, along with cognitive impairment (Biessels & Despa, 2018).

Findings on T2D-induced brain alterations vary by study, but span atrophy, including of the hippocampus, the structure responsible for memory and learning, as well as lacunae, infarcts, white matter hyperintensities, and microbleeds (Biessels & Despa, 2018). Simultaneously with these structural changes observable by magnetic resonance imaging (MRI), T2D patients are predisposed to developing cognitive impairments and dementia (Biessels & Despa, 2018). The precise mechanisms remain incompletely understood and are likely multifactorial (Biessels & Despa, 2018; Henn et al., 2022) but may involve peripheral hyperglycemia and brain insulin resistance (Kullmann et al., 2016) impacting brain glucose metabolism (Biessels et al., 2020), vascular dysfunction and impaired blood flow (Biessels et al., 2020; Wang et al., 2021), inflammation (Biessels et al., 2020), oxidative stress (Barone et al., 2021; Groeneveld et al., 2019) and mitochondrial dysfunction (Pinti et al., 2019), and altered neurotransmitter levels (Thielen et al., 2019; van Bussel et al., 2016). As an essential energy substrate, brain uptake and utilization of glucose occur in an insulin-independent manner; however, since insulin exerts various effects in the brain, such as regulating neurotransmitter receptor expression and localization and metabolism more broadly (Arnold et al., 2018), growing insulin resistance can impact brain glucose and neurochemical profiles.

Most studies of the brain in vivo under T2D conditions have examined structural and functional changes by MRI. However, these studies do not generate mechanistic insight on altered brain metabolism, which is highly relevant to a metabolic state, such as T2D. Positron emission tomography using radiolabeled ^{18}F-fluorodeoxyglucose can potentially assess brain glucose metabolism in vivo in the context of T2D (Biessels et al., 2020), but is limited to the single metabolite. Proton magnetic resonance spectroscopy (^{1}H MRS) is a non-invasive technique that facilitates simultaneous measurements of several metabolite levels in vivo in both human and animal tissue (Sherry et al., 2015).

Using in vivo ^{1}H MRS at high magnetic field (9.4 T), we (Wang et al., 2012) and others (Duarte et al., 2009) have shown the effects of acute and chronic hyperglycemia on neurochemical profiles of animal models with streptozotocin (STZ)-induced type 1 diabetes (T1D). Non-invasive longitudinal monitoring of metabolites by ^{1}H MRS reveals alterations in brain metabolism in T1D with time (Wang et al., 2012), underscoring the potential benefit of the technique as a surrogate of disease progression. Moreover, investigating the pathogenesis of diabetes on the brain in terms of glucose and other metabolic pathways could potentially lead to the development of new treatment strategies for mitigating cognitive impairment. In animal models of T2D, ^{1}H MRS similarly demonstrates diabetes-induced changes in hippocampal metabolite and neurochemical profiles, such as in the *db/db* mouse model (Zheng, Zheng, Zhao et al., 2017), Zucker diabetic fatty rats (van der Graaf et al., 2004), and lean Goto-Kakizaki rats (Duarte et al., 2018).

Despite significant interest and research into neurochemical profiles in the diabetic brain, to the best of our knowledge, no longitudinal ^{1}H MRS analysis has been conducted to delineate the shorter- and longer-term effects of T2D on brain metabolism and neurochemical profiles in animal models. To address this knowledge gap, we launched the present study that we first employed clinical ^{1}H MRS at 3 T to measure neurochemical profiles of 12 metabolites in T2D patients, identifying differential levels in four metabolites, glucose, *myo*-inositol, taurine, and choline-containing compounds. Using higher magnetic field ^{1}H MRS at 9.4 T, we then characterized neurochemical profiles of 20 metabolites in *db/db* mice, a model with deficient leptin signaling, which replicates human T2D, including hyperglycemia, insulin resistance, and frequent comorbid obesity. Profiling suggested differential hippocampus and striatum levels in *db/db* versus control *db+* littermates in ascorbate, creatine, phosphocreatine, γ-aminobutyric acid (GABA), glucose, glutamate, glutamine, glutathione, glycerophosphoryl-choline, lactate, *myo*-inositol, and taurine, which longitudinal analysis suggests persisted with chronic disease progression. Overall, our study demonstrates the utility of ^{1}H MRS as a non-invasive tool for characterizing and monitoring metabolic changes with T2D progression in the brain.

2 | METHODS

2.1 | Human participants

Nineteen participants with T2D and 17 closely age- and sex-matched healthy controls (Figure 1a) were examined according to the study protocol approved by the Human Subjects Committee at the University of Kansas Medical Center (approval numbers HSC11066 and HSC11119) and registered at the ClinicalTrials.gov (NCT NCT00845130). T2D patients were recruited from the Cray Diabetes Clinic and other clinics at the University of Kansas Medical Center, and the Greater Kansas City area and provided written informed consent for participating in the study. All participants had a definite diagnosis of T2D (type 2 per WHO definition) for at least 3 years. Although most T2D patients (16 out of 17) were on antidiabetic medications (Table 1), their diabetes remained poorly controlled, and they continued to experience hyperglycemia and elevated HbA1c (≥7.5%). Individuals with a history of other diseases, head injury, claustrophobia, or other unstable medical conditions,

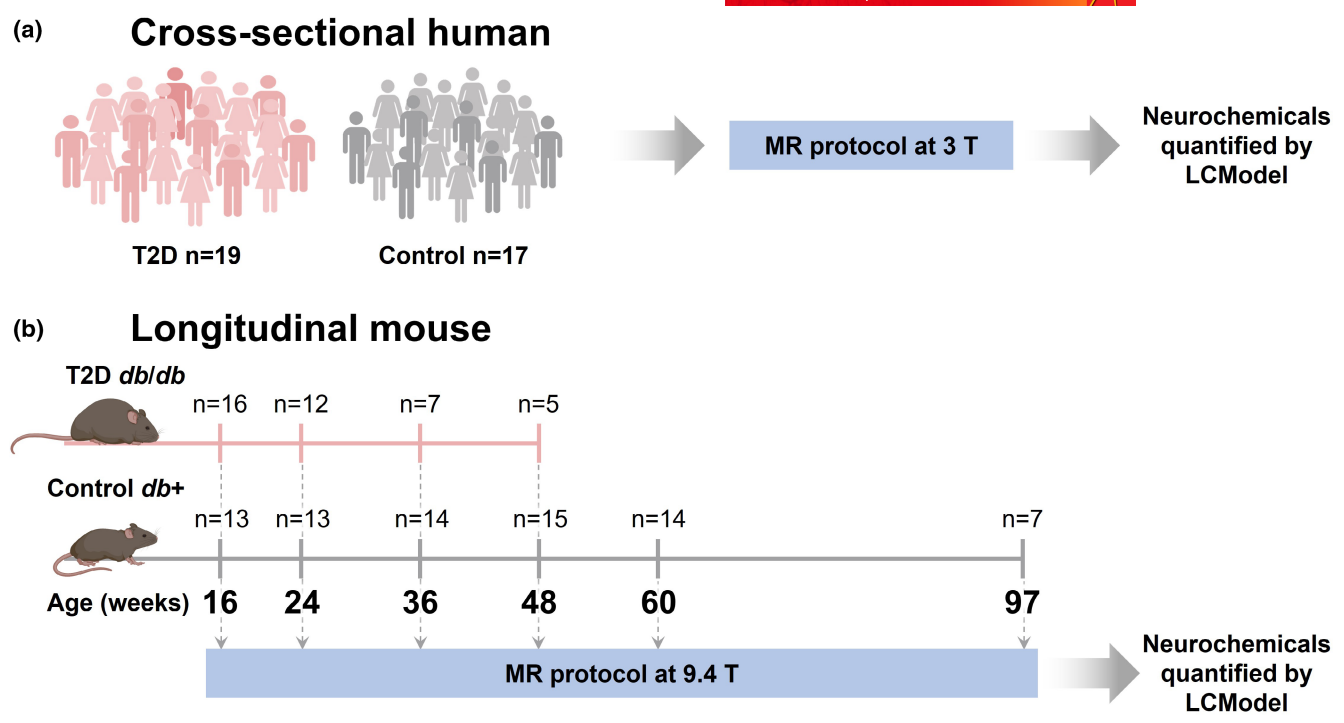


FIGURE 1 Overview of study design. (a) Cross-sectional human study of patients with type 2 diabetes (T2D) and age- and sex-matched control participants assessed by MR at 3 T. (b) Longitudinal mouse study of T2D (*db*/*db*) and control (*db*+) mice assessed by MR at 9.4 T at the indicated ages. Created, in part, in Biorender.com.

TABLE 1 Participant demographics.

Characteristic	Control ($n=17$)	T2D ($n=19$)	*p*-value
Sex			
Female, *n* (%)	11 (64.7%)	11 (57.9%)	
Male, *n* (%)	6 (35.3%)	8 (42.1%)	
Age, years	45.4 ± 6.7	47.4 ± 5.8	0.33
Diabetes duration, years		7.6 ± 2.8	
Baseline BMI, kg/m^2	25.4 ± 1.7	30.7 ± 2.7	<0.00001
HbA1c, %	5.4 ± 0.4	9.3 ± 1.9	<0.00001
Fasting plasma glucose, mg/dL	91.9 ± 12.7	191.2 ± 69.2	<0.00001
Antidiabetic treatment[a]			
Metformin		14	
Insulin		10	
Other (e.g., sulfonylureas, glitazones)		8	
None		1	

Note: All values represented as mean ± standard deviation. A two-tailed *t*-test was used to compare age, BMI, HbA1c and plasma glucose. BMI, body mass index; HbA1c, hemoglobin A1c.

[a]Some T2D participants were taking multiple antidiabetic medications.

chronic inflammatory conditions, or concurrent neurological diseases except for mild diabetic autonomic or peripheral neuropathy were excluded.

2.2 | MR protocols for human studies at 3 T

All MR scans of human participants were performed on a 3 T clinical MR system (Allegra, VA25, Siemens, Erlangen, Germany). A custom-built quadrature radiofrequency (RF) helmet coil, a partial volume transmit/receive coil, was used to provide a relatively homogeneous RF field and high sensitivity with volume coverage above the eyes (Choi et al., 2007). After positioning the participant supine in the magnet, three-plane scout MR images were acquired using a gradient echo sequence to locate the volume of interest (VOI). The VOI, a 2-cm axial slab for the ^{1}H MR chemical shift imaging (CSI), was positioned to cover the area above the corpus callosum, including the frontal to parietal regions, and located in the iso-center of the magnet (Figure 2a, top left). Localized automated shimming was performed to optimize static magnetic field homogeneity in the CSI slice using field map-based shimming. The shimming routine adjusts all first- and second-order shim currents based on measured field maps. This shimming improves magnetic field homogeneity across the complete CSI slice, resulting in <7 Hz full width at half-maximum of the water line width in the $6\times6\times2\,cm^3$ volume in the CSI slice. ^{1}H MR CSI was acquired using a Point-Resolved Spectroscopy CSI sequence (repetition time (TR)/echo time (TE) = 2000/30 ms, field of view = $20\times20\,cm^2$, VOI = $10\times12\times2\,cm^3$, matrix size = 12×12) with vendor-provided three CHEmical Shift Selective water suppression and outer volume suppression methods. Following the ^{1}H MR CSI, high-resolution T_1-weighted MRI was performed

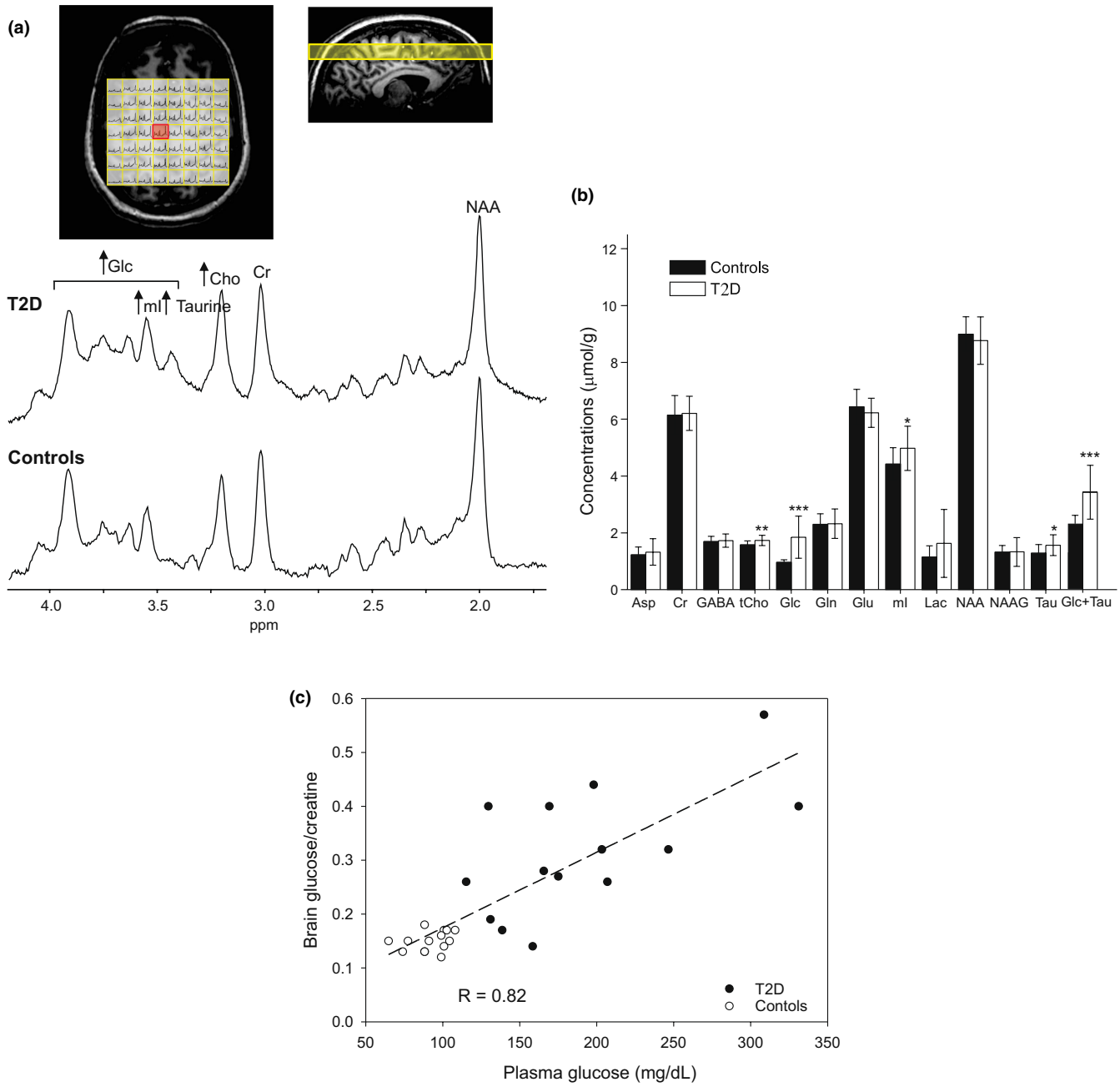


FIGURE 2 MRS spectra and metabolite quantification in cross-sectional human study. (a) Positioning of the ^{1}H CSI slab (top, right, yellow box) and MR spectra overlaid on MRI (top, left). A red box in MRI indicates the location of voxel where the representative spectra were extracted. Brain ^{1}H MRS spectra from T2D (top) and healthy control (bottom) participants measured at 3 T (TE = 30 ms, TR = 2 s, nominal voxel size = 1.25 × 1.25 × 2.0 cm^3). (b) Quantification of 12 metabolite concentrations in T2D patients (n = 19) versus healthy controls (n = 17). All spectra were quantified using LCModel. Data presented as the mean ± one standard deviation. A two-tailed t-test compared neurochemical concentrations, except a Mann–Whitney U-test compared glucose and taurine, because they correlated significantly in LCModel (*p < 0.05; **p < 0.01; ***p < 0.001). (c) Linear relationship between brain glucose and plasma glucose concentrations in poorly controlled T2D patients (n = 14) versus healthy controls (n = 13). Asp, aspartate; Cr, total creatine (creatine and phosphocreatine); GABA, γ-aminobutyric acid; tCho, total choline; Glc, glucose; Gln, glutamine; Glu, glutamate; mI, *myo*-inositol; Lac, lactate; NAA, N-acetylaspartate; NAAG, N-acetylaspartylglutamate; Tau, taurine; TE, echo time; TR, repetition time.

using the Magnetization Prepared Rapid Acquisition Gradient Echo (MPRAGE) sequence (TR/TE = 1700/4.38 ms, inversion time = 700 ms, field of view = 176 × 192 × 120 with 1 mm^3 isotropic resolution) to correct the effect of brain atrophy on metabolite quantification.

2.3 | MR data analysis and quantification of 3T data

Neurochemical profiles in human participants were measured in the frontoparietal regions because of high B0 homogeneity,

which results in reliable quantification of metabolite levels. CSI was measured because it provides better chemical shift displacement error versus single-voxel MRS. Human ^{1}H MR CSI data were processed by spatial reconstruction following spatial filtering and zero-padding to the 16×16 final matrix size with a nominal voxel size of 1.25×1.25×2 cm^3 using Siemens software and exported to an external workstation for further offline processing. The CSI data quantification of metabolite concentrations was performed using LCModel (linear combination of model spectra of metabolite solutions in vitro, version 5.1-7 W) (Provencher, 1993). Unsuppressed water signals acquired from the same VOI were used to calculate the concentrations of 12 metabolites, including aspartate, total choline-containing compounds (mainly glycerophosphoryl-choline and phosphorylcholine), total creatine (creatine and phosphocreatine), γ-aminobutyric acid (GABA), glucose, glutamine, glutamate, lactate, *myo*-inositol, N-acetylaspartate (NAA), N-acetylaspartylglutamate (NAAG), and taurine. Glycerophosphoryl-choline and phosphorylcholine were quantified together as total choline-containing compounds, and creatine and phosphocreatine were quantified together as total creatine because a 3 T field does not provide sufficient spectral dispersion to differentiate them.

Metabolite concentrations at each CSI voxel were corrected for brain atrophy using high-resolution T_1-weighted MR images (Choi et al., 2006). Briefly, the process of correcting for brain atrophy involved co-registration of high-resolution T_1-weighted MR images with CSI data, segmentation of T_1-weighted MRI, application of slice profiles of VOI to segmented MRI, down-sampling of segmented MRI, and Fourier transformation of segmented MRI. The final neurochemical concentrations at each voxel were calculated by dividing the tissue fraction value of uncorrected concentration values from LCModel with the water reference. No relaxation correction was performed. The final concentration of each metabolite in the frontoparietal region including both gray and white matter was obtained by averaging metabolite concentration values with Cramer-Rao lower bound of 40% or less in central 6×6 voxels. An unpaired two-tailed t-test assuming equal variances was performed to compare mean metabolite levels in T2D versus healthy controls except for glucose and taurine, whose values correlated because of signal overlap at 3 T. Glucose and taurine levels were compared using a non-parametric test (Mann–Whitney U-test) between the two groups. *p*-values less than 0.05 were considered significant.

2.4 | Animals

Procedures in this study were performed according to the guidelines for the care and use of laboratory animals at the University of Kansas Medical Center. The study was approved by the Institutional Animal Care and Use Committee (approval number 2012–1905). The study included 16 male BKS.Cg-m+/+Leprdb/J (*db/db*) mice (Figure 1b), homozygous for a spontaneous mutation to the leptin receptor, versus 13 male non-diabetic littermate (*db*+) controls (Strain #:000642, Jackson Laboratory, Bar Harbor, Maine, USA). *db/db* mice become obese at approximately 3–4 weeks of age and develop elevated blood glucose levels at 4 to 8 weeks, resulting in consistently high blood glucose levels (>33.4 mmol/L) longitudinally with time versus *db*+ mice (9–14 mmol/L) (Bogdanov et al., 2014; Davis et al., 2010; De Gregorio et al., 2018; O'Brien et al., 2014). The animals were maintained on a 12-h light/dark cycle and had free access to water and chow during the entire study duration.

In vivo MRS and MRI measurements were performed on all animals longitudinally at up to 6 time points, starting at 16 weeks of age (n=16 *db/db*, n=13 *db*+) and then at 24 weeks of age (n=12 *db/db*, n=13 *db*+), 36 weeks of age (n=7 *db/db*, n=14 *db*+), 48 weeks of age (n=5 *db/db*, n=15 *db*+), 60 weeks of age (n=14 *db*+), and 97 weeks of age (n=7 *db*+). Only a few *db/db* mice survived up to 48 weeks because they die earlier from diabetic complications. Six additional *db*+ mice from 36 weeks and later were added to increase the sample size and compensate the loss of animals at later ages for longitudinal scans of up to 97 weeks. Likewise, six additional *db/db* mice from 36 weeks and later were added to increase the sample size and compensate the loss of animals at later ages for longitudinal scans of up to 48 weeks.

For MR scans, anesthesia was optimized by monitoring oxygenation, heart rate, and respiratory rate and selecting the minimum level needed to keep animals sedated while affecting physiology to the smallest extent possible. Animals were anesthetized in an induction chamber filled with a gas mixture of air and oxygen (ratio=2:1 with 4% vaporized isoflurane). Animals were then positioned prone in an acrylic sled, and heads were secured using a bite bar and head holder. The isoflurane level was maintained at 1–2% to keep animals anesthetized throughout the MR experiments. A blanket with circulating warm water maintained animal body temperature at 37±0.5°C, which was verified by a rectal thermo-sensor (Cole-Parmer, Vernon Hills, IL, USA). A pulse oximeter (Starr Life Sciences, Oakmont, PA, USA) monitored animal blood oxygenation and heart rate, which were 98.0±2.6% and 431±66 bpm, respectively. An air pillow placed under the animal and connected to a physiological monitoring system monitored animal respiratory rate (SA Instruments, Stony Brook, NY, USA). A glucose oxidase method (Accu-Chek Active system, Roche Diagnostic, Switzerland) measured non-fasting glucose level in blood, collected by tail pin prick performed under light isoflurane anesthesia, before and after MR scans.

2.5 | MR protocols for animal studies at 9.4 T

All mouse MR scans were performed on a 9.4 T Varian INOVA MR system (Varian, Palo Alto, CA, USA) equipped with gradient coils (40 G/cm, 250 μs) of 12 cm inner diameter and shim coils with maximum second-order shim strength of 0.4 G/cm^2 (Magnex Scientific, Abingdon, UK). The animal head was fixed by a nose cone with a two-loop quadrature RF surface coil placed on top of the head to

transmit and receive at 400 MHz frequency. The two-loop quadrature coil was geometrically decoupled, and each loop was 18 mm in diameter. T_2-weighted fast spin-echo images (echo train length = 16, echo spacing/TE/TR = 11/11/4000 ms, matrix size = 256 × 256, field of view = 25.6 × 25.6 mm^2, slice thickness = 0.5 mm, number of averages = 2) were acquired to assess morphological changes.

T_2-weighted images were used to localize a spectroscopic voxel of 4–6 μL in a volume in the hippocampus and striatum. The hippocampus and striatum were selected because of relatively higher B0 homogeneity versus cortex, which, in mouse, resides close to the air–tissue boundary, reducing B0 homogeneity because of the magnetic susceptibility effect. Magnetic field inhomogeneity in the VOI was adjusted using FASTMAP (Gruetter, 1993), and the water signal was suppressed using variable power RF pulses with optimized relaxation delays (VAPOR) technique (Tkác et al., 1999). The spin-echo, full-intensity acquired localized (SPECIAL) spectroscopy (TE = 3 ms, TR = 4 s, 2048 complex points acquired, number of averages = 320–640 depending on the voxel size) (Mlynárik et al., 2006) combined with outer volume suppression was used, resulting in a full width at half-maximum of the unsuppressed water signal in the range of 12–15 Hz.

2.6 | MR data analysis and quantification of 9.4 T data

T_2-weighted images were used to study morphological changes in brain atrophy in both animal groups from 16 to 48 weeks of age. Changes in the volume of the whole brain, ventricles, and hippocampus were quantified by manually drawing regions of interest (ROIs) within each slice of the corresponding region (Figure 3) displayed in NIH ImageJ software (Schneider et al., 2012). The volumes of marked ROIs were computed by summing their voxels using the ImageJ ROI manager tool. The total number of pixels in each ROI was used for volumetric information. Cortical thickness was calculated by averaging thickness measurements at three different locations in the dorsal cortical area (indicated by bars in Figure 3).

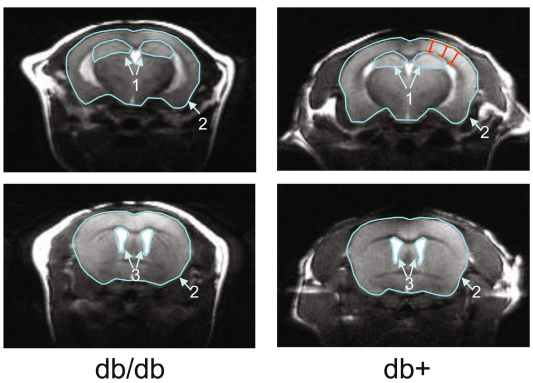


FIGURE 3 MRI images and volume/thickness quantification in longitudinal mouse study. Morphological measurements at age 48 weeks, overlaid on T_2-weighted fast spin-echo images (echo train length = 16, echo spacing/TE/TR = 11/11/4000 ms, matrix size = 256 × 256, FOV = 25.6 × 25.6 mm^2, slice thickness = 0.5 mm, number of averages = 2). Measurements of morphological changes include hippocampal volume (1), whole brain volume (2), ventricle volume (3), and cortical thickness (red bars) in the dorsal cortical area. FOV, field of view; TE, echo time; TR, repetition time.

Acquired MRS signals were corrected for frequency drift based on the creatine peak at 3.02 ppm within each block (16 free induction decay signals) of the data set. Then, all MRS data were averaged and corrected for residual eddy current effects using a reference water signal collected for each VOI. Unsuppressed water signals acquired from the same VOI were used as an internal reference to estimate metabolite concentrations by analyzing spectra in the frequency domain using LCModel, like the human data. In the analysis, the in vivo spectra were fitted by a superposition of a set of basis spectra using a constrained regularization algorithm.

For quantifying the concentration of each metabolite, LCModel analyses generated a Cramer-Rao lower bound value to represent the precision of the concentration estimations. In this study, only metabolites with Cramer-Rao lower bound values ≤30% were used for statistical analysis. Thus, out of a total of 21 metabolites measured, 20 with Cramer-Rao lower bound values ≤30% were quantified in the hippocampus and striatum of *db/db* and *db+* mice, including alanine, ascorbate, aspartate, glycerophosphoryl-choline, phosphorylcholine, creatine, phosphocreatine, GABA, glucose, glutamine, glutamate, glutathione, *myo*-inositol, lactate, NAA, NAAG, phosphorylethanolamine, serine, taurine, and macromolecules. *Beta*-hydroxybutyrate was measured but not included in further analysis since it had Cramer-Rao lower bound values >30%.

2.7 | Statistical analysis

Statistical analyses were performed using R statistical software (version 4.2.3; R Foundation for Statistical Computing, Vienna, Austria). Linear mixed-effects models with Tukey's post hoc corrections were used to compare individual metabolite levels and brain volume measures between *db/db* versus *db+* mice at different age groups, which effectively address varying sample sizes because of missing data points in repeated measures. Normality was assessed by Q-Q plots, and all results are presented in Files S1–S3. *p*-values from post hoc tests of genotype for each age group were cross-adjusted using the Benjamini–Hochberg method. A two-step hypothesis testing approach was used to compare individual metabolite levels between *db/db* versus *db+* mice at different age groups (Chi & Muller, 2013). First, principal component scores were computed based on the metabolite profile data, summarizing the overall variability in the dataset. Next, these principal component scores were compared between *db/db* versus *db+* mice groups using MANOVA (multivariate analysis of variance).

3 | RESULTS

For the cross-sectional human clinical study, demographic information shows body mass index, fasting plasma glucose, and HbA1c

values were higher in T2D patients, consistent with poorly controlled hyperglycemia (Table 1). Representative MR spectra of T2D versus control participants, acquired from the frontoparietal region by ^{1}H MRS imaging, show excellent spectral quality, facilitating quantification of 12 metabolites (Figure 2a; Figure S1). As a result of significant spectral overlap between the glucose and taurine signals at 3T, whose correlation coefficient of the LCModel indicated was −0.35±0.4, we included glucose+taurine as an outcome. On the other hand, gray matter fraction values within the analyzed brain region did not differ between groups (52.3±3.4% for T2D vs. 54.5±5.4% for controls, $p=0.2$); thus, the effect of tissue composition on measured neurochemical concentrations is expected to be negligible. Four out of the 12 metabolites were significantly elevated in the brain of T2D participants versus age- and sex-matched controls, glucose (91%, $p<0.001$), taurine (22%, $p=0.02$), glucose+taurine (56%, $p<0.001$), *myo*-inositol (12%, $p=0.02$), and total choline-containing compounds (10%, $p=0.01$) (Figure 2b). Brain glucose concentrations exhibited a linear relationship with plasma glucose levels (Figure 2c, $R=0.82$, $p=0.00001$). Brain and plasma glucose levels in T2D participants were 2.06-fold and 2.08-fold higher, respectively, versus controls. Plasma glucose and HbA1c also correlated with choline, *myo*-inositol, and taurine, while body mass index did not correlate with neurochemical concentrations.

For the longitudinal animal study, *db/db* mice were scanned from 16 to 48 weeks of age, while *db+* mice were scanned from 16 to 97 weeks of age. Measurements at each time point included MR images and MR spectra as well as blood glucose levels. At 36 weeks of age, average blood glucose level of *db/db* mice was 550 mg/dL, which was 131% higher than average blood glucose level of their *db+* counterparts.

From MR images, brain morphological changes were assessed by quantifying brain volume, hippocampal volume, ventricle volume, and cortical thickness using ROI analysis (Figure 3). The most prominent differences between the two groups were brain volumes, which were 9%–13% smaller in *db/db* versus *db+* mice ($p<0.0001$; Table 2); however, brain volumes of both animal groups were relatively constant with age, varying less than 2% from 16 to 48 weeks of age and did not change significantly (File S1). Hippocampal volume differed significantly between the two groups ($p=0.0002$), and there were no significant differences in ventricle volume ($p=0.4446$). Cortical thickness of *db/db* mice was significantly thinner by 10%–13% versus *db+* mice ($p<0.0001$); moreover, cortical thickness in both groups decreased non-significantly with age.

In MR spectra, glucose signals in the mouse brain were clearly observable at 5.23 ppm because of excellent water suppression in ^{1}H MRS at 9.4 T (Figure 4a, hippocampus; Figure 5a, striatum). Among 20 metabolites, 17 metabolites were selected for longitudinal plots based on the reliability of quantification using LCModel (Figure 4b, hippocampus; Figure 5b, striatum). Brain glucose signal intensities indicated clear elevated hippocampal and striatal glucose in *db/db* versus *db+* mice, consistent with elevated blood glucose levels in *db/db* mice. Additionally, in *db/db* versus *db+* mice, hippocampal and striatal ascorbate, creatine, phosphocreatine, GABA, glutamate, glutamine, glycerophosphoryl-choline, *myo*-inositol, and taurine were higher, whereas lactate was lower. Glutathione was also elevated in the hippocampus of *db/db* versus *db+* mice, but was only at the margin of significance in the striatum. Furthermore, serine was elevated in the hippocampus and NAA elevated in the striatum of *db/db* versus *db+* mice. The fold-change differences of all measured metabolites between the *db/db* and *db+* groups at 16, 24, 36, and 48 weeks of age in the hippocampus and striatum are shown in Figure S2.

We observed a few longitudinal changes in neurochemicals (Files S2 and S3). In the hippocampus, glycerophosphoryl-choline generally

TABLE 2 Structural MRI metrics in mouse brain.

Age (week)	Animal	Brain volume (mm^3)	Hippocampal volume (mm^3)	Ventricle volume (mm^3)	Cortical thickness (mm)
	p-value	**<0.0001**	**0.0002**	0.4446	**<0.0001**
16	*db+*	151.5±4.5	6.30±0.55	2.46±0.76	0.70±0.01
	db/db	134.2±9.2	4.96±0.62	2.56±2.42	0.63±0.04
24	*db+*	151.3±5.4	6.18±1.43	2.31±0.62	0.71±0.05
	db/db	137.4±7.2	4.85±0.86	3.01±2.28	0.62±0.05
36	*db+*	152.4±5.8	6.18±0.80	2.42±0.73	0.70±0.03
	db/db	137.4±3.9	5.04±0.69	3.30±1.53	0.60±0.03
48	*db+*	151.9±4.2	5.75±0.68	2.88±1.44	0.68±0.04
	db/db	131.0±10.0	5.27±0.19	2.72±1.84	0.60±0.04

Note: Changes in brain volume, hippocampal volume, ventricle volume, and cortex thickness. Linear mixed-effects model analyzed statistical significance; plots annotated with *p*-value for *db/db* versus *db+* comparison; *p*-values for temporal trend in File S1; 16 weeks of age ($n=16$ *db/db*, $n=10$ *db+*), 24 weeks of age ($n=12$ *db/db*, $n=11$ *db+*), 36 weeks of age ($n=8$ *db/db*, $n=14$ *db+*), 48 weeks of age ($n=4$ *db/db*, $n=15$ *db+*), 60 weeks of age ($n=17$ *db+*), and 97 weeks of age ($n=16$ *db+*). Please note that the number of animals varied at each age because of missing measurements or loss/addition of animals to compensate the lost animals, and the statistical analysis method could effectively address varying number of samples in longitudinal measures. Bold indicates significant differences between *db/db* and *db+* mice.

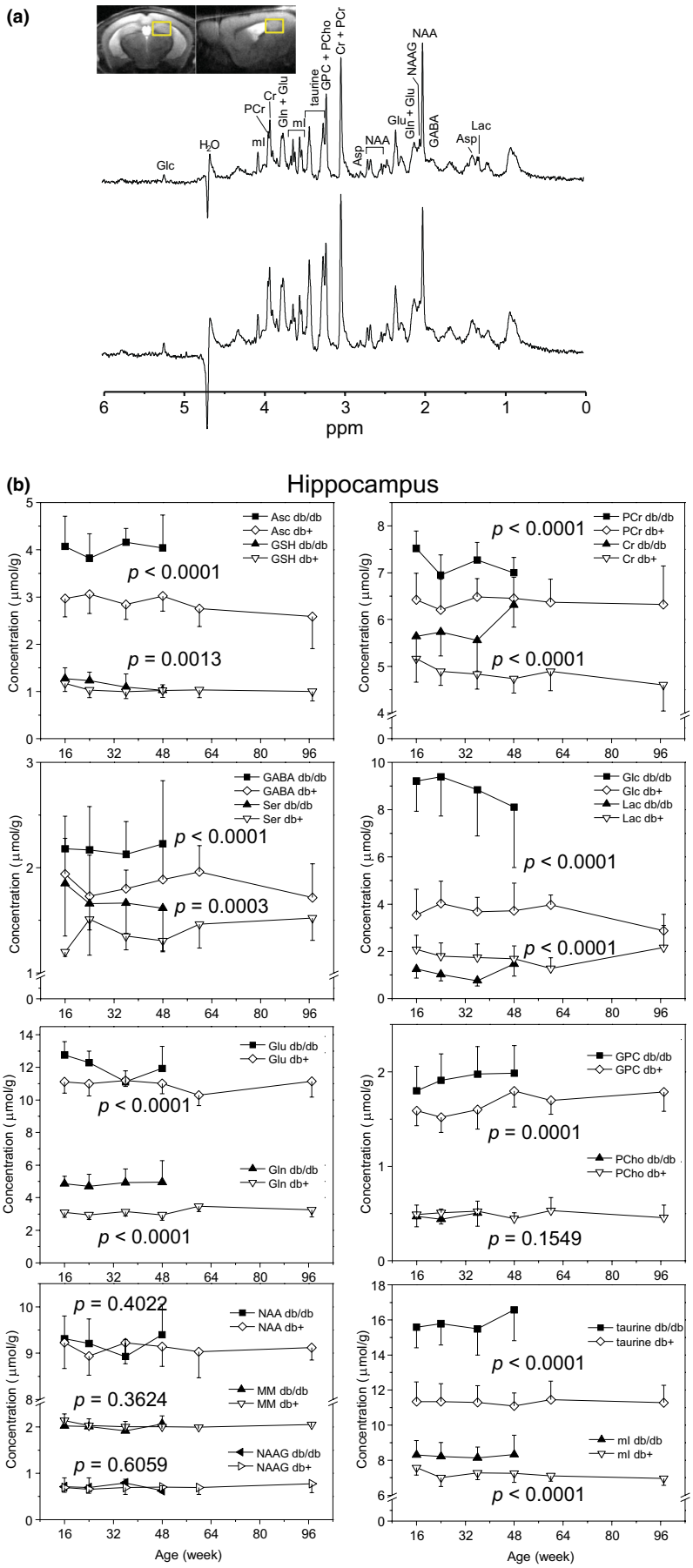


FIGURE 4 Hippocampal MRS spectra and metabolite quantification in longitudinal mouse study. (a) A typical voxel placed over the hippocampus region (inset), and spectra acquired from the hippocampal voxel of diabetic *db/db* (bottom) versus non-diabetic control *db+* (top) mice at 16 weeks of age. Note that ascorbate (Asc), glutathione (GSH) and serine (Ser) are not labeled in MR spectra as these signals are buried under other overlapping signals with high intensity. (b) Longitudinal comparison of hippocampal metabolite concentrations in *db/db* (black) versus *db+* (white) mice. Data presented as the mean ± one standard deviation. Linear mixed-effects model analyzed statistical significance; plots annotated with *p*-value for *db/db* versus *db+* comparison; *p*-values for temporal trend in File S2; n for groups in Figure 1.

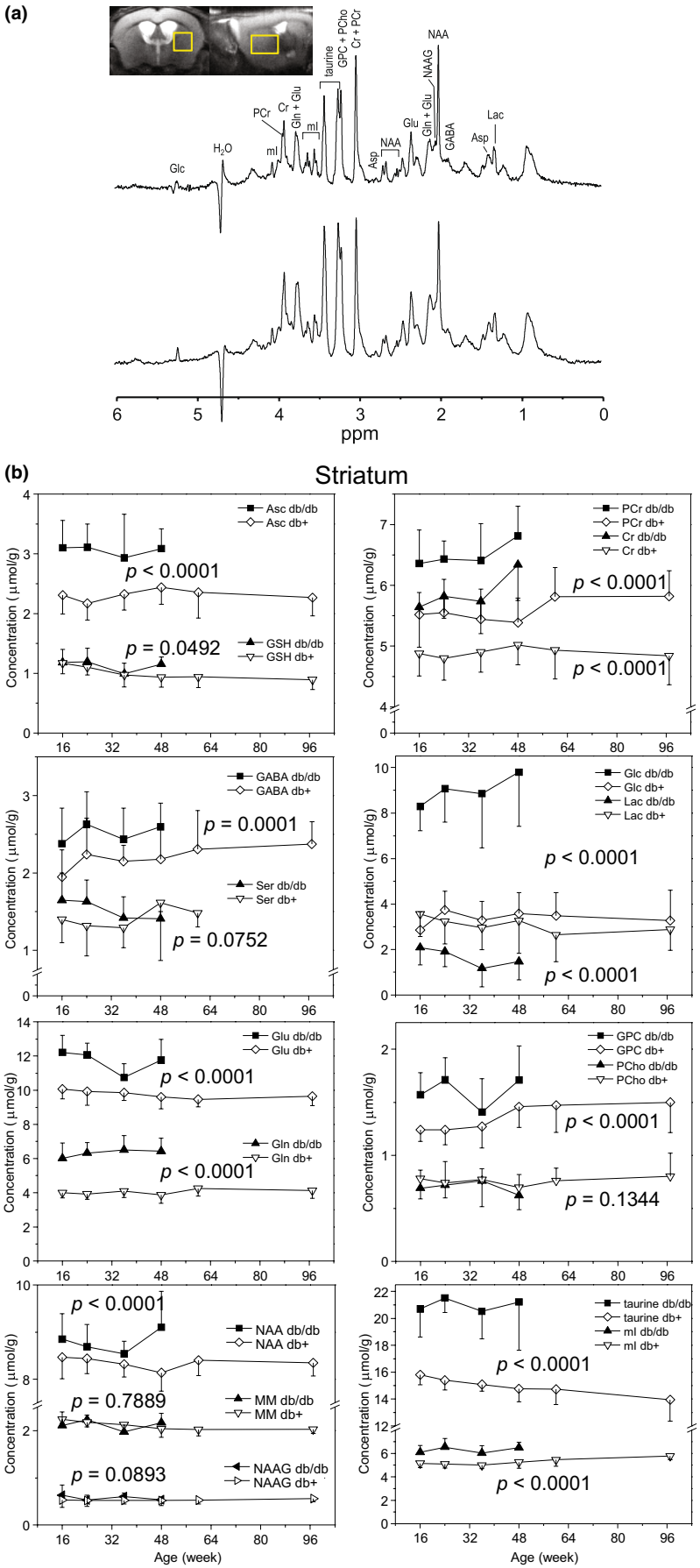


FIGURE 5 Striatal MRS spectra and metabolite quantification in longitudinal mouse study. (a) A typical voxel placed over the striatum region (inset), and spectra acquired from the hippocampal voxel of diabetic *db/db* (bottom) versus non-diabetic control *db+* (top) mice at 16 weeks of age. (b) Longitudinal comparison of striatal metabolite concentrations in *db/db* (black) versus *db+* (white) mice. Data presented as the mean ± one standard deviation. Linear mixed-effects model analyzed statistical significance; plots annotated with *p*-value for *db/db* versus *db+* comparison; *p*-values for temporal trend in File S3; n for groups in Figure 1. Asc, ascorbate; Asp, aspartate; Cr, creatine; GABA, γ-aminobutyric acid; Glc, glucose; Gln, glutamine; Glu, glutamate; GPC, glycerophosphoryl-choline; GSH, glutathione; mI, *myo*-inositol; Lac, lactate; MM, macromolecules; NAA, N-acetylaspartate; NAAG, N-acetylaspartylglutamate; PCho, phosphorylcholine; PCr, phosphocreatine; Ser, serine.

increased with time in both *db/db* and *db+* mice, which pooled post hoc analysis found was significant between 16 versus 48 weeks and 24 versus 48 weeks. Glutathione levels dropped subtly with time in the hippocampus of both *db/db* and *db+* mice, but was only significant between 16 versus 36 weeks and 16 versus 48 weeks by pooled post hoc analysis. Hippocampal phosphocreatine also varied with time, with significant differences occurring between 16 versus 24 weeks. In the striatum, more neurochemicals varied with time in *db/db* and/or *db+* mice, with longitudinal changes in glucose (significant between 16 and 48 weeks), glycerophosphoryl-choline (significant between 16 and 48 weeks, 36 and 48 weeks), glutathione (significant between 16 and 36 weeks, 16 and 48 weeks, 24 and 36 weeks), and *myo*-Inositol (significant between 36 and 48 weeks). Striatal glutamate levels dropped subtly but significantly overall between the earliest and latest time point, although this effect interacted with *db/db* versus *db+* group effects. Neurochemical profiles of *db/db* mice remained distinct overall from those of *db+* mice with aging.

We next addressed the ability of metabolic markers to differentiate disease status (T2D versus non-diabetic) by principal component analysis. Plotting the first and second principal components at each time point, 16, 24, 36, and 48 weeks, significantly separated *db/db* from *db+* mice (Figure 6), indicating distinct neurochemical profiles in the T2D versus non-diabetic state. Most of the variance in the first and second principal components could be attributed to glucose and taurine at all time points, suggesting they contributed most to the distinction between *db/db* from *db+* mice (Table S1). Glutamate and glutamine also contributed frequently among the top four significant contributors. Overall, the principal component analysis indicates distinct metabolic patterns by diabetes status.

4 | DISCUSSION

This study presents the effects of poorly controlled hyperglycemia in T2D, defined as HbA1c ≥ 7.5%, on neurochemicals in cross-sectional analysis in humans as well as longitudinal analysis in an animal model of T2D, *db/db* mice. Here, ^{1}H MRS at 3 T facilitated measurements for a neurochemical profile of 12 metabolites, finding differences in four metabolites, in the frontoparietal regions of T2D patients versus healthy control participants. Brain glucose levels correlated positively with plasma glucose. The use of the higher magnetic field of 9.4 T in the longitudinal animal study allowed characterization of a 20-metabolite panel in the hippocampus and striatum with the increased sensitivity and high-resolution MR images enabled to quantify brain volumes. Most metabolites were elevated in the hippocampus and striatum of *db/db* mice versus control *db+* littermates, including ascorbate, creatine, phosphocreatine, GABA, glucose, glutamate, glutamine, glycerophosphoryl-choline, *myo*-inositol, and taurine. Lactate, on the other hand, was deficient in *db/db* mice relative to *db+* counterparts. Longitudinal measurements showed changes in some metabolites in *db/db* mice and *db+* controls with aging, and metabolic and neurochemical differences between diabetic and non-diabetic mice persisted with disease progression. In tandem with these metabolic changes, *db/db* mice exhibited brain atrophy, especially in total brain volume, relative to *db+* controls.

In our cross-sectional human clinical study, 4 out of 12 metabolites differed in the frontoparietal regions of T2D patients versus control participants, which included glucose, *myo*-inositol, taurine, and choline-containing compounds, all elevated, as well as the composite glucose+taurine. Brain glucose in T2D patients has not been widely investigated using ^{1}H MRS. Of the studies we found, one reported elevated glucose across multiple brain regions in T2D (Sinha et al., 2014), whereas another noted a blunted response to the occipital lobe glucose uptake in T2D patients during hyperglycemia induction (target plasma glucose 220 mg/dL) (Hwang et al., 2017). Glucose entry into the brain is facilitated primarily by insulin-independent glucose transporter 1 (GLUT1) (Rebelos et al., 2021); therefore, at baseline, T2D patients might be expected to exhibit elevated brain glucose entry because of elevated plasma glucose. Indeed, we noted a positive correlation between brain and plasma glucose. However, a blunted brain entry response in T2D to extreme glucose challenge may be a protective or countering mechanism to limit excessive entry.

Meta-analysis and systematic review of several studies of T2D participants examined cumulative evidence for *myo*-inositol and choline (Wu et al., 2017; Zhao et al., 2018). *myo*-Inositol levels were significantly higher in the frontal white matter in T2D patients (Ajilore et al., 2007; Li et al., 2020), but other studies noted no differences (Wu et al., 2017). Regarding choline, the net evidence suggests elevated total choline-containing compound concentrations in the cortex (Li et al., 2020) and choline to creatine ratios (Wu et al., 2017), though some studies have noted no differences in cortical and subcortical nuclei regions (Ajilore et al., 2007; Sinha et al., 2014). Differential brain taurine in T2D, to our knowledge, is a novel finding, although a small study of pediatric patients with T1D and diabetic ketoacidosis reported elevated brain taurine (Cameron et al., 2005). Taurine, along with *myo*-inositol and choline, are organic osmolytes that help maintain cellular volume under hyperosmotic conditions, as would occur during hyperglycemia (Burg & Ferraris, 2008). A recent study showed that taurine supplementation prevented high-fat diet (HFD)-associated hippocampal alterations and memory impairment, suggesting a neuroprotective role of taurine in addition to its role as an osmotic regulator (Garcia-Serrano, Vieira et al., 2022). Indeed, taurine serves important roles in nervous tissue, exerting antioxidant effects and regulating calcium signaling (Ripps & Shen, 2012). Similarly, *myo*-inositol is a secondary messenger with numerous functions in nervous tissue, such as calcium homeostasis, DNA and RNA biology, and synaptic membrane trafficking (Fisher et al., 2002). Choline is a critical component of cell membranes and acetylcholine neurotransmitter (Blusztajn et al., 2017). Thus, elevated levels in these neurochemicals are likely to exert multifactorial effects in the T2D brain.

We did not detect altered brain GABA levels in T2D patients, though some literature reports higher concentrations of GABA in the medial prefrontal cortex (Thielen et al., 2019) and occipital region (van Bussel et al., 2016) of T2D patients. The studies also

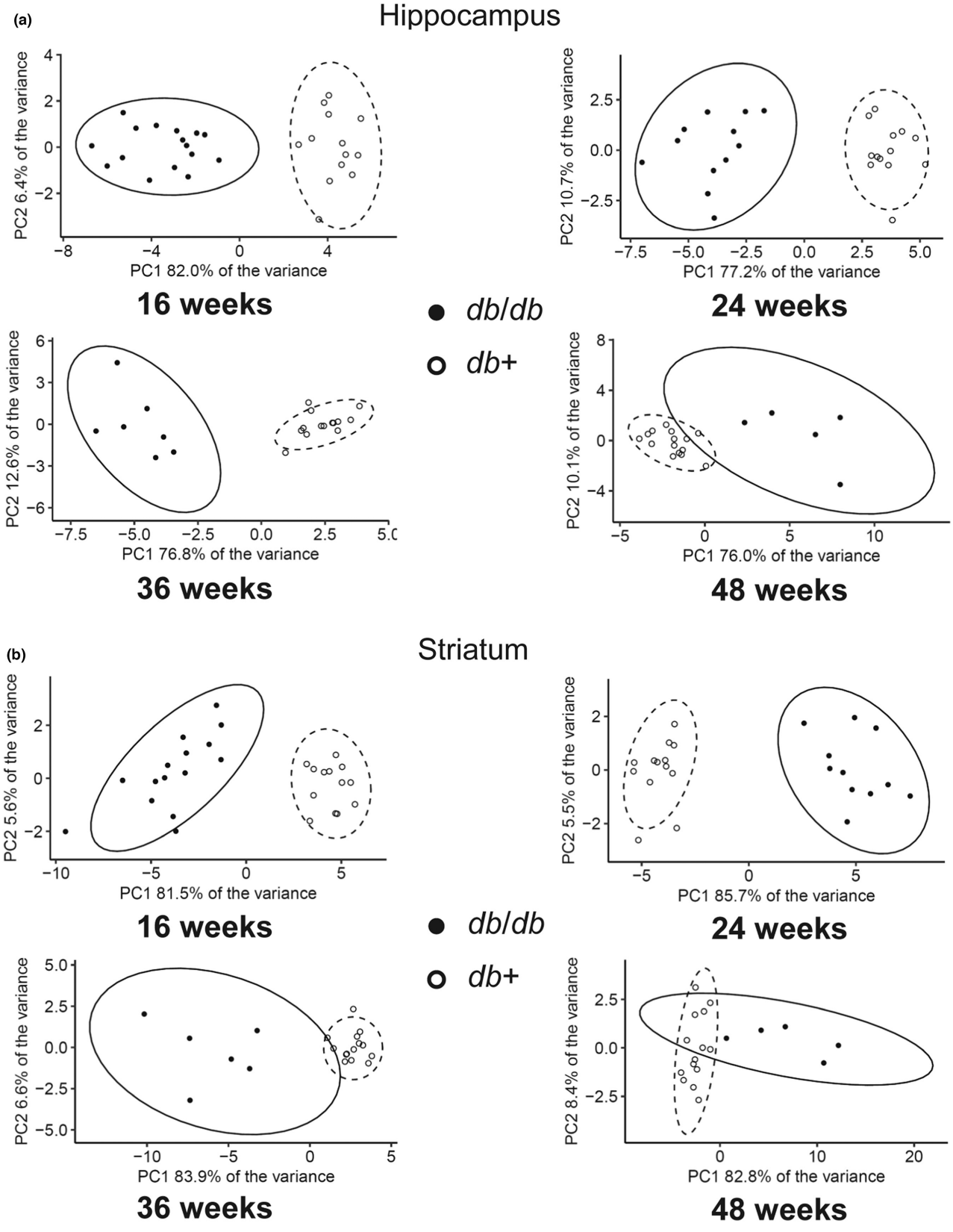


FIGURE 6 Neurochemical profiles differentiate T2D *db/db* from control *db+* mice. Principal component analysis scatter plot of the first and second principal components for *db/db* (black) versus *db+* (white) mice in (a) hippocampus and (b) striatum. Ellipses represent 95% confidence region for each group, *db/db* (solid) versus *db+* (dotted), based on the principal components, assuming a bivariate normal distribution. Across all time points and in both hippocampus and striatum, metabolite profiles of *db/db* and *db+* mice differed significantly by MANOVA, $p < 0.0001$ for all.

found a negative correlation, with elevated GABA linked to lower cognitive performance (Thielen et al., 2019; van Bussel et al., 2016). Glutamate, the predominant excitatory neurotransmitter, and glutamine did not differ in our cohort of diabetic and non-diabetic study participants, aligned with one study (Ajilore et al., 2007) but not another, which noted higher glutamate and glutamine levels in the white matter of T2D (Sinha et al., 2014). In addition to its role as an amino acid in protein synthesis and energy substrate, glutamine helps recycle glutamate as part of the astrocytic glutamine–glutamate or glutamine–glutamate/GABA cycles, which support neuronal synaptic transmission (Bélanger et al., 2011; Henn et al., 2022; Walls et al., 2015).

Likewise, we did not find differential NAA levels in the brain of T2D patients, in agreement with some reports (Ajilore et al., 2007; Wu et al., 2017), but not with others that found lower levels (Li et al., 2020; Lu et al., 2019; Sinha et al., 2014). NAA is an osmolyte, bioenergetic molecule, and a source for myelin and neuronal dipeptide NAAG synthesis (Moffett et al., 2007). NAA is also widely regarded as a marker of neuronal viability and integrity. Finally, in our human clinical data, we also found no differences in creatine levels, in agreement with one study (Sinha et al., 2014). Creatine together with phosphocreatine serves as an energy buffer system for generating ATP under energetically demanding conditions.

In our longitudinal mouse study, we employed the well-established animal model of T2D, *db/db* mouse, which develops T2D because of a spontaneous mutation to the leptin receptor. Although based on a mutation, which differs from humans, the *db/db* mouse mirrors many phenotypes of human diabetes, including hyperglycemia, glucose intolerance, and insulin resistance, as well as frequently comorbid obesity and dyslipidemia (Burke et al., 2017; Guest & Rahmoune, 2019; Hinder et al., 2019). Indeed, our T2D patients in this study had a mean body mass index of 30.7 kg/m^2, which is within the obesity range. Moreover, the *db/db* mouse develops diabetic complications, akin to humans, including cognitive decline (Zheng, Zheng, Wang et al., 2017; Zheng, Zheng, Zhao et al., 2017). Using structural MRI, we first quantified volumetric changes to various brain regions, finding, most notably, atrophy in total brain volume in *db/db* versus *db+* mice, aligned with brain atrophy in human studies (Biessels et al., 2020; Biessels & Despa, 2018).

For the mouse study at 9.4 T, we could quantify 20 neurochemicals in the hippocampus and striatum compared to 12 in human scans at 3 T, because of the better sensitivity and spectral dispersion. Of the four metabolites that were elevated in the frontoparietal regions of T2D patients, similar findings were observed in the hippocampus and striatum of *db/db* mice at all time points. Like the human clinical data, we noted elevated hippocampal and striatal glucose, *myo*-inositol, and taurine in the *db/db* mouse brain. Although there were few studies in the literature that detected elevated taurine in humans, this finding in the *db/db* mouse brain is much better characterized (Zheng et al., 2016; Zheng, Zheng, Zhao et al., 2017). A very recent study with a different HFD-STZ-induced T2D model reported elevated cortical taurine in T2D HFD mice compared to obese HFD mice (Caramelo et al., 2023). Brain taurine is also elevated in hyperglycemic STZ-induced T1D rats (Chandrasekaran et al., 2020; Duarte et al., 2009). As a potentially neuroprotective molecule (Li et al., 2019; Wu et al., 2020), elevated brain taurine may be a counter measure to hyperglycemia-induced neuronal damage. Moreover, the diabetic mouse condition had elevated glycerophosphoryl-choline, which, as the most abundant choline-containing compound in the brain, likely reflects elevated total choline-containing compounds in our human data.

Additionally in diabetic mice, we noted elevated brain glutamate and glutamine and GABA at specific time points. This is partly in agreement with the human literature; some studies reported elevated GABA with unchanged glutamate and glutamine under the diabetic condition (Thielen et al., 2019; van Bussel et al., 2016), whereas another study noted higher glutamate and glutamine in T2D patients without reporting findings regarding GABA (Sinha et al., 2014). For animal studies, a series of reports in the T2D *db/db* model at 17 weeks of age indicated higher glutamine and lower glutamate and GABA (Zheng et al., 2016; Zheng, Zheng, Zhao et al., 2017) in the hippocampus, which isotope labeling attributed to impaired whole neurotransmitter metabolism and breakdown in neuron–astrocyte cooperation linked to cognitive impairment in the diabetic condition (Zheng, Zheng, Wang et al., 2017). This is reinforced by a similar experiment in Goto-Kakizaki rats, a lean T2D model based on selective inbreeding for insulin resistance and insulin secretion defects. [1,6-^{13}C]-glucose infusion uncovers markedly diminished glutamate–glutamine cycling in the brain (encompassing hippocampus, thalamus, striatum, and part of the cortex), along with impaired glutamine synthesis and mitochondrial tricarboxylic acid metabolism, in Goto-Kakizaki versus control rats aged between 6 and 7 months (Girault et al., 2019). Elevated hippocampal glutamine was recorded in T2D HFD-STZ mice versus lean standard-diet fed controls aged 20 weeks following 10 weeks of diet, but no differences were seen in glutamate nor GABA (Caramelo et al., 2023).

Overall, there is a lack of consensus regarding brain GABA, glutamate, and glutamine levels in the T2D context, possibly arising from analyzed brain area, that is, cortex versus hippocampus or striatum, gray or white matter, diabetes duration, glycemic control, that is, well-controlled (Thielen et al., 2019; van Bussel et al., 2016) versus poorly controlled (Sinha et al., 2014) diabetes as well as disease severity, for example, HbA1c (van Bussel et al., 2016), experimental methodology, for example, ex vivo (Zheng et al., 2016; Zheng, Zheng, Wang et al., 2017; Zheng, Zheng, Zhao et al., 2017) versus in vivo (Caramelo et al., 2023; Girault et al., 2019) tissue analysis, acquisition during fasted (Girault et al., 2019; Zheng, Zheng, Wang et al., 2017) versus non-fasted condition, and whether the analysis corrected for brain volume, that is, atrophy.

In *db/db* mice, we observed elevated creatine and phosphocreatine in the hippocampus and striatum. The former, creatine, remain unchanged in humans (Sinha et al., 2014); however, since mouse studies were conducted at 9.4 T, creatine and phosphocreatine could be quantified separately, which is highly challenging in human spectra even at 7 T, making direct comparisons difficult. We did not note differential hippocampal NAA levels in *db/db* versus *db+* mice,

although NAA may have been elevated in the striatum. Hippocampal findings are aligned with the human frontoparietal findings from the present study, but not with our prior work in the cortex and hippocampus of an T1D STZ rat model (Wang et al., 2012) or a literature report in *db/db* mouse hippocampus extract, possibly due to *post-mortem* changes (Zheng, Zheng, Zhao et al., 2017). Literature in T2D patients is mixed (Ajilore et al., 2007; Li et al., 2020; Lu et al., 2019; Sinha et al., 2014; Wu et al., 2017). The discrepancy may arise from disease duration, since NAA did not decrease significantly in T1D rats until prolonged hyperglycemic conditions (Wang et al., 2012); however, further investigation is needed to determine precise reasons.

When we examined temporal trends in neurochemical profiles, we found changes spanning a few metabolites, including glucose, glutamate, glutathione, glycerophosphoryl-choline, phosphocreatine, and *myo*-inositol in *db/db* and/or *db+* mice in the hippocampus and/or striatum. This contrasts with our prior investigation of T1D rats, which found more defined evolution in metabolite levels with diabetes progression (Wang et al., 2012). These differences possibly reflect disease stage, that is, earlier versus later disease status, and model-specific etiologies, with insulin deficiency in STZ-induced T1D and leptin receptor deficiency in T2D *db/db*.

In addition to variation between individual metabolites, we used principal component analysis to examine whether neurochemical profiles were distinct in the diabetic versus control conditions. Indeed, *db/db* mice clustered separately from *db+* mice at all time points, across 16, 24, 36, and 48 weeks, suggestive of differences over the diabetic disease course compared to healthy controls. The distinction could be primarily attributed to glucose and taurine.

This study has several limitations; the human data are cross-sectional and relatively small, although this is an issue for many published studies. The small cohort size restricted our ability to examine correlations beyond diabetes status, such as glycemic, insulin sensitivity, and obesity metrics as well as analysis by sex. Regarding the animal model, although *db/db* mice recapitulate the essential features of human T2D, the etiology is based on deficient leptin signaling, which is distinct from the scenario in humans and may confound results. Moreover, the *db/db* model also develops obesity, which may introduce confounding from the effects of dysregulated lipids in the brain.

Several studies have examined neurochemical profiles across various brain regions in HFD (Caramelo et al., 2023;Lizarbe et al., 2018; Ribeiro et al., 2018) and high-fat and high-sucrose diet (Garcia-Serrano, Mohr et al., 2022) rodent models. HFD rodents develop obesity as well as insulin resistance and elevated blood glucose not meeting the formal criteria for diabetes. The HFD rodent brain is characterized by altered creatine, creatine/phosphocreatine, NAA, NAAG, glutathione, *myo*-inositol, taurine, total choline, phosphorylethanolamine, glucose, lactate (Lizarbe et al., 2018), glutamate, and glutamine (Ribeiro et al., 2018) variably in different regions, including the hippocampus, cortex, caudate–putamen, and hypothalamus. However, interestingly, many changes track with glucose intolerance and elevated blood glucose levels (Lizarbe et al., 2018; Ribeiro et al., 2018), suggestive of a contribution of hyperglycemia to the neurochemical profiles in these obese HFD models. Similarly, neurochemical profiles differ subtly in obese HFD mice versus HFD with STZ-induced T2D, indicative of influences from diabetic hyperglycemia. Overall, these changes may be related to neurometabolic pathways related to glucose. However, future studies will be needed to fully disentangle the contributions of hyperglycemia and dyslipidemia to metabolic alterations in the brain in the context of T2D. Finally, our mouse study employed only male *db/db* and *db+* mice; since sex differences occur in T2D (Kautzky-Willer et al., 2023) and the T2D brain (Espeland et al., 2020), this was a significant shortcoming and suggests that further longitudinal investigation should include both male and female cohorts. Indeed, hypothalamic neurochemical profiles may subtly differ in male versus female obese HFD mice (Campillo et al., 2022), advocating examination by sex in the T2D context.

This study also has some strengths; the mouse analysis was longitudinal, and, since ^{1}H MRS is non-invasive, examined hippocampal and striatal neurochemical profiles in the same cohort of animals as they progressed in their disease course. This lowered the natural variation present in animals, enhancing our ability to detect brain metabolic changes within the same animals. Moreover, the high-field spectra in the mouse study enhanced sensitivity and spectral dispersion, allowing simultaneous quantification of 17 metabolites.

In summary, our results provide insight into the effect of poorly controlled chronic hyperglycemia from T2D on neurochemical profiles in human frontoparietal regions and mouse hippocampus and striatum using in vivo ^{1}H MRS. In addition to elevated brain glucose concentrations, hyperglycemia led to significant concentration changes in neurochemicals that serve a suite of biological functions, including as neurotransmitters, bioenergetic substrates, organic osmolytes, messenger molecules, and various additional roles. Principal component analysis of neurochemical profiles demonstrate reliable separation of the diabetic group from controls with disease progression. Overall, the animal T2D *db/db* model could reflect neurochemical alterations observed in poorly controlled T2D in humans and enable further characterization of the disease longitudinally.

AUTHOR CONTRIBUTIONS

In-Young Choi: Conceptualization; funding acquisition; methodology; resources; supervision; writing – original draft; writing – review and editing. **Wen-Tung Wang:** Formal analysis; methodology; visualization; writing – original draft. **Bhumsoo Kim:** Conceptualization; writing – original draft; writing – review and editing. **Junguk Hur:** Formal analysis; visualization; writing – review and editing. **David C. Robbins:** Conceptualization; methodology; resources. **Dae-Gyu Jang:** Formal analysis; visualization; writing – review and editing. **Masha G. Savelieff:** Visualization; writing – original draft; writing – review and editing. **Eva L. Feldman:** Conceptualization; funding acquisition; resources; writing – original draft; writing – review and

editing. **Phil Lee:** Conceptualization; formal analysis; methodology; visualization; writing – original draft; writing – review and editing.

ACKNOWLEDGMENTS

The authors thank Dr. Jo Ann Lierman for assistance in the human clinical study and the participants for taking part in the study.

All experiments were conducted in compliance with the ARRIVE guidelines.

CONFLICT OF INTEREST STATEMENT

In-Young Choi is a Guest Editor of the special issue "Energetics and cognition in aging brain: Impact of substrates and microbiome". The authors declare no further potential conflict of interest.

FUNDING INFORMATION

Funding support includes the National Institutes of Health (R21DK081079, M01RR023940 to IYC; R01DK130913, R01DK129320, R01DK107956 to ELF), the Juvenile Diabetes Research Foundation (5COE-2019-861-S-B to ELF), and the Andrea and Lawrence A. Wolfe Brain Health Initiative, the Robert and Katherine Jacobs Environmental Health Initiative, the Robert E. Nederlander Sr. Program for Alzheimer's Research, the Sinai Medical Staff Foundation Research on Studying Diet and Brain Health, the Nathan and Rose Milstein Research Fund, and the NeuroNetwork for Emerging Therapies.

DATA AVAILABILITY STATEMENT

Data available on request from the authors.

ORCID

In-Young Choi https://orcid.org/0000-0002-1489-4119
Masha G. Savelieff https://orcid.org/0000-0001-5575-2494
Eva L. Feldman https://orcid.org/0000-0002-9162-2694
Phil Lee https://orcid.org/0000-0002-2087-8887

REFERENCES

Ahmad, E., Lim, S., Lamptey, R., Webb, D. R., & Davies, M. J. (2022). Type 2 diabetes. *Lancet*, *400*(10365), 1803–1820. https://doi.org/10.1016/s0140-6736(22)01655-5

Ajilore, O., Haroon, E., Kumaran, S., Darwin, C., Binesh, N., Mintz, J., Miller, J., Thomas, M. A., & Kumar, A. (2007). Measurement of brain metabolites in patients with type 2 diabetes and major depression using proton magnetic resonance spectroscopy. *Neuropsychopharmacology*, *32*(6), 1224–1231. https://doi.org/10.1038/sj.npp.1301248

Arnold, S. E., Arvanitakis, Z., Macauley-Rambach, S. L., Koenig, A. M., Wang, H. Y., Ahima, R. S., Craft, S., Gandy, S., Buettner, C., Stoeckel, L. E., Holtzman, D. M., & Nathan, D. M. (2018). Brain insulin resistance in type 2 diabetes and Alzheimer disease: Concepts and conundrums. *Nature Reviews. Neurology*, *14*(3), 168–181. https://doi.org/10.1038/nrneurol.2017.185

Barone, E., Di Domenico, F., Perluigi, M., & Butterfield, D. A. (2021). The interplay among oxidative stress, brain insulin resistance and AMPK dysfunction contribute to neurodegeneration in type 2 diabetes and Alzheimer disease. *Free Radical Biology & Medicine*, *176*, 16–33. https://doi.org/10.1016/j.freeradbiomed.2021.09.006

Bélanger, M., Allaman, I., & Magistretti, P. J. (2011). Brain energy metabolism: Focus on astrocyte-neuron metabolic cooperation. *Cell Metabolism*, *14*(6), 724–738. https://doi.org/10.1016/j.cmet.2011.08.016

Biessels, G. J., & Despa, F. (2018). Cognitive decline and dementia in diabetes mellitus: Mechanisms and clinical implications. *Nature Reviews. Endocrinology*, *14*(10), 591–604. https://doi.org/10.1038/s41574-018-0048-7

Biessels, G. J., Nobili, F., Teunissen, C. E., Simó, R., & Scheltens, P. (2020). Understanding multifactorial brain changes in type 2 diabetes: A biomarker perspective. *Lancet Neurology*, *19*(8), 699–710. https://doi.org/10.1016/s1474-4422(20)30139-3

Blusztajn, J. K., Slack, B. E., & Mellott, T. J. (2017). Neuroprotective actions of dietary choline. *Nutrients*, *9*(8), 815. https://doi.org/10.3390/nu9080815

Bogdanov, P., Corraliza, L., Villena, J. A., Carvalho, A. R., Garcia-Arumí, J., Ramos, D., Ruberte, J., Simó, R., & Hernández, C. (2014). The *db/db* mouse: A useful model for the study of diabetic retinal neurodegeneration. *PLoS One*, *9*(5), e97302. https://doi.org/10.1371/journal.pone.0097302

Burg, M. B., & Ferraris, J. D. (2008). Intracellular organic osmolytes: Function and regulation. *The Journal of Biological Chemistry*, *283*(12), 7309–7313. https://doi.org/10.1074/jbc.R700042200

Burke, S. J., Batdorf, H. M., Burk, D. H., Noland, R. C., Eder, A. E., Boulos, M. S., Karlstad, M. D., & Collier, J. J. (2017). db/db mice exhibit features of human type 2 diabetes that are not present in weight-matched C57BL/6J mice fed a Western diet. *Journal Diabetes Research*, *2017*, 8503754. https://doi.org/10.1155/2017/8503754

Cameron, F. J., Kean, M. J., Wellard, R. M., Werther, G. A., Neil, J. J., & Inder, T. E. (2005). Insights into the acute cerebral metabolic changes associated with childhood diabetes. *Diabetic Medicine*, *22*(5), 648–653. https://doi.org/10.1111/j.1464-5491.2005.01453.x

Campillo, B. W., Galguera, D., Cerdan, S., López-Larrubia, P., & Lizarbe, B. (2022). Short-term high-fat diet alters the mouse brain magnetic resonance imaging parameters consistently with neuroinflammation on males and metabolic rearrangements on females. A pre-clinical study with an optimized selection of linear mixed-effects models. *Frontiers in Neuroscience*, *16*, 1025108. https://doi.org/10.3389/fnins.2022.1025108

Caramelo, B., Monteiro-Alfredo, T., Martins, J., Sereno, J., Castelhano, J., Manadas, B., Castelo-Branco, M., & Matafome, P. (2023). Functional imaging and neurochemistry identify in vivo neuroprotection mechanisms counteracting excitotoxicity and neurovascular changes in the hippocampus and visual cortex of obese and type 2 diabetic animal models. *Journal of Neurochemistry*, *165*(6), 892–906. https://doi.org/10.1111/jnc.15825

Chandrasekaran, K., Choi, J., Arvas, M. I., Salimian, M., Singh, S., Xu, S., Gullapalli, R. P., Kristian, T., & Russell, J. W. (2020). Nicotinamide mononucleotide administration prevents experimental diabetes-induced cognitive impairment and loss of hippocampal neurons. *International Journal of Molecular Sciences*, *21*(11), 3756. https://doi.org/10.3390/ijms21113756

Chi, Y. Y., & Muller, K. E. (2013). Two-step hypothesis testing when the number of variables exceeds the sample size. *Communications in Statistics: Simulation and Computation*, *42*(5), 1113–1125. https://doi.org/10.1080/03610918.2012.659819

Choi, I.-Y., Lee, S.-P., Garwood, M., Ugurbil, K., & Merkle, H. (2007). Simple partial volume transceive coils for *in vivo* ^{1}H MR studies at high magnetic fields. *Concepts in Magnetic Resonance Part B: Magnetic Resonance Engineering*, *31B*(2), 71–85.

Choi, I.-Y., Lee, S. P., Merkle, H., & Shen, J. (2006). *In vivo* detection of gray and white matter differences in GABA concentration in the human brain. *NeuroImage*, *33*(1), 85–93. https://doi.org/10.1016/j.neuroimage.2006.06.016

Davis, R. C., Castellani, L. W., Hosseini, M., Ben-Zeev, O., Mao, H. Z., Weinstein, M. M., Jung, D. Y., Jun, J. Y., Kim, J. K., Lusis, A. J., & Péterfy, M. (2010). Early hepatic insulin resistance precedes the onset of diabetes in obese C57BLKS-db/db mice. *Diabetes*, *59*(7), 1616–1625. https://doi.org/10.2337/db09-0878

De Gregorio, C., Contador, D., Campero, M., Ezquer, M., & Ezquer, F. (2018). Characterization of diabetic neuropathy progression in a mouse model of type 2 diabetes mellitus. *Biology Open*, *7*(9), bio036830. https://doi.org/10.1242/bio.036830

Duarte, J. M., Carvalho, R. A., Cunha, R. A., & Gruetter, R. (2009). Caffeine consumption attenuates neurochemical modifications in the hippocampus of streptozotocin-induced diabetic rats. *Journal of Neurochemistry*, *111*(2), 368–379. https://doi.org/10.1111/j.1471-4159.2009.06349.x

Duarte, J. M. N., Skoug, C., Silva, H. B., Carvalho, R. A., Gruetter, R., & Cunha, R. A. (2018). Impact of caffeine consumption on type 2 diabetes-induced spatial memory impairment and neurochemical alterations in the hippocampus. *Frontiers in Neuroscience*, *12*, 1015. https://doi.org/10.3389/fnins.2018.01015

Elafros, M. A., Andersen, H., Bennett, D. L., Savelieff, M. G., Viswanathan, V., Callaghan, B. C., & Feldman, E. L. (2022). Towards prevention of diabetic peripheral neuropathy: Clinical presentation, pathogenesis, and new treatments. *Lancet Neurology*, *21*(10), 922–936. https://doi.org/10.1016/s1474-4422(22)00188-0

Espeland, M. A., Hayden, K. M., Lockhart, S. N., Yassine, H. N., Hoscheidt, S., Yasar, S., Luchsinger, J. A., Neiberg, R. H., Diaz Brinton, R., & Carmichael, O. (2020). Sex-related differences in brain volumes and cerebral blood flow among overweight and obese adults with type 2 diabetes: Exploratory analyses from the action for health in diabetes brain magnetic resonance imaging study. *The Journals of Gerontology. Series A, Biological Sciences and Medical Sciences*, *75*(4), 771–778. https://doi.org/10.1093/gerona/glz090

Fisher, S. K., Novak, J. E., & Agranoff, B. W. (2002). Inositol and higher inositol phosphates in neural tissues: Homeostasis, metabolism and functional significance. *Journal of Neurochemistry*, *82*(4), 736–754. https://doi.org/10.1046/j.1471-4159.2002.01041.x

Garcia-Serrano, A. M., Mohr, A. A., Philippe, J., Skoug, C., Spégel, P., & Duarte, J. M. N. (2022). Cognitive impairment and metabolite profile alterations in the hippocampus and cortex of male and female mice exposed to a fat and sugar-rich diet are normalized by diet reversal. *Aging and Disease*, *13*(1), 267–283. https://doi.org/10.14336/ad.2021.0720

Garcia-Serrano, A. M., Vieira, J. P. P., Fleischhart, V., & Duarte, J. M. N. (2022). Taurine and N-acetylcysteine treatments prevent memory impairment and metabolite profile alterations in the hippocampus of high-fat diet-fed female mice. *Nutritional Neuroscience*, *1-13*, 1090–1102. https://doi.org/10.1080/1028415x.2022.2131062

Girault, F. M., Sonnay, S., Gruetter, R., & Duarte, J. M. N. (2019). Alterations of brain energy metabolism in type 2 diabetic Goto-Kakizaki rats measured *in vivo* by ^{13}C magnetic resonance spectroscopy. *Neurotoxicity Research*, *36*(2), 268–278. https://doi.org/10.1007/s12640-017-9821-y

Groeneveld, O. N., van den Berg, E., Johansen, O. E., Schnaidt, S., Hermansson, K., Zinman, B., Espeland, M. A., & Biessels, G. J. (2019). Oxidative stress and endothelial dysfunction are associated with reduced cognition in type 2 diabetes. *Diabetes & Vascular Disease Research*, *16*(6), 577–581. https://doi.org/10.1177/1479164119848093

Gruetter, R. (1993). Automatic, localized *in vivo* adjustment of all first- and second-order shim coils. *Magnetic Resonance in Medicine*, *29*(6), 804–811. https://doi.org/10.1002/mrm.1910290613

Guest, P. C., & Rahmoune, H. (2019). Characterization of the *db/db* mouse model of type 2 diabetes. *Methods in Molecular Biology*, *1916*, 195–201. https://doi.org/10.1007/978-1-4939-8994-2_18

Henn, R. E., Noureldein, M. H., Elzinga, S. E., Kim, B., Savelieff, M. G., & Feldman, E. L. (2022). Glial-neuron crosstalk in health and disease: A focus on metabolism, obesity, and cognitive impairment. *Neurobiology of Disease*, *170*, 105766. https://doi.org/10.1016/j.nbd.2022.105766

Hinder, L. M., Sas, K. M., O'Brien, P. D., Backus, C., Kayampilly, P., Hayes, J. M., Lin, C. M., Zhang, H., Shanmugam, S., Rumora, A. E., Abcouwer, S. F., Brosius, F. C., 3rd, Pennathur, S., & Feldman, E. L. (2019). Mitochondrial uncoupling has no effect on microvascular complications in type 2 diabetes. *Scientific Reports*, *9*(1), 881. https://doi.org/10.1038/s41598-018-37376-y

Hwang, J. J., Jiang, L., Hamza, M., Sanchez Rangel, E., Dai, F., Belfort-DeAguiar, R., Parikh, L., Koo, B. B., Rothman, D. L., Mason, G., & Sherwin, R. S. (2017). Blunted rise in brain glucose levels during hyperglycemia in adults with obesity and T2DM. *JCI Insight*, *2*(20), e95913. https://doi.org/10.1172/jci.insight.95913

Kautzky-Willer, A., Leutner, M., & Harreiter, J. (2023). Sex: Differences in type 2 diabetes. *Diabetologia*, *66*(6), 986–1002. https://doi.org/10.1007/s00125-023-05891-x

Kullmann, S., Heni, M., Hallschmid, M., Fritsche, A., Preissl, H., & Häring, H. U. (2016). Brain insulin resistance at the crossroads of metabolic and cognitive disorders in humans. *Physiological Reviews*, *96*(4), 1169–1209. https://doi.org/10.1152/physrev.00032.2015

Li, K., Shi, X., Luo, M., Inam, U. L., Wu, P., Zhang, M., Zhang, C., Li, Q., Wang, Y., & Piao, F. (2019). Taurine protects against myelin damage of sciatic nerve in diabetic peripheral neuropathy rats by controlling apoptosis of schwann cells via NGF/Akt/GSK3β pathway. *Experimental Cell Research*, *383*(2), 111557. https://doi.org/10.1016/j.yexcr.2019.111557

Li, S., Yin, C., Zhao, W., Lian, X., & Hong, Q. (2020). Application of hydrogen proton magnetic resonance technology combined with brain neurometabolite analysis in the treatment of cognitive impairment caused by type 2 diabetes mellitus. *World Neurosurgery*, *138*, 654–662. https://doi.org/10.1016/j.wneu.2019.12.162

Lizarbe, B., Soares, A. F., Larsson, S., & Duarte, J. M. N. (2018). Neurochemical modifications in the hippocampus, cortex and hypothalamus of mice exposed to long-term high-fat diet. *Frontiers in Neuroscience*, *12*, 985. https://doi.org/10.3389/fnins.2018.00985

Lu, X., Gong, W., Wen, Z., Hu, L., Peng, Z., & Zha, Y. (2019). Correlation between diabetic cognitive impairment and diabetic retinopathy in patients with T2DM by ^{1}H-MRS. *Frontiers in Neurology*, *10*, 1068. https://doi.org/10.3389/fneur.2019.01068

Mlynárik, V., Gambarota, G., Frenkel, H., & Gruetter, R. (2006). Localized short-echo-time proton MR spectroscopy with full signal-intensity acquisition. *Magnetic Resonance in Medicine*, *56*(5), 965–970. https://doi.org/10.1002/mrm.21043

Moffett, J. R., Ross, B., Arun, P., Madhavarao, C. N., & Namboodiri, A. M. (2007). N-Acetylaspartate in the CNS: From neurodiagnostics to neurobiology. *Progress in Neurobiology*, *81*(2), 89–131. https://doi.org/10.1016/j.pneurobio.2006.12.003

O'Brien, P. D., Sakowski, S. A., & Feldman, E. L. (2014). Mouse models of diabetic neuropathy. *ILAR Journal*, *54*(3), 259–272. https://doi.org/10.1093/ilar/ilt052

Pinti, M. V., Fink, G. K., Hathaway, Q. A., Durr, A. J., Kunovac, A., & Hollander, J. M. (2019). Mitochondrial dysfunction in type 2 diabetes mellitus: An organ-based analysis. *American Journal of Physiology. Endocrinology and Metabolism*, *316*(2), E268–e285. https://doi.org/10.1152/ajpendo.00314.2018

Provencher, S. W. (1993). Estimation of metabolite concentrations from localized *in vivo* proton NMR spectra. *Magnetic Resonance in Medicine*, *30*(6), 672–679. https://doi.org/10.1002/mrm.1910300604

Rebelos, E., Rinne, J. O., Nuutila, P., & Ekblad, L. L. (2021). Brain glucose metabolism in health, obesity, and cognitive decline-does insulin have anything to do with it? A narrative review. *Journal of Clinical Medicine*, *10*(7), 1532. https://doi.org/10.3390/jcm10071532

Ribeiro, M., Castelhano, J., Petrella, L. I., Sereno, J., Rodrigues, T., Neves, C., Letra, L., Baptista, F. I., Seiça, R., Matafome, P., & Castelo-Branco,

M. (2018). High-fat diet induces a neurometabolic state characterized by changes in glutamate and N-acetylaspartate pools associated with early glucose intolerance: An in vivo multimodal MRI study. *Journal of Magnetic Resonance Imaging*, *48*, 757–766. https://doi.org/10.1002/jmri.25942

Ripps, H., & Shen, W. (2012). Review: Taurine: A "very essential" amino acid. *Molecular Vision*, *18*, 2673–2686.

Sabanayagam, C., Banu, R., Chee, M. L., Lee, R., Wang, Y. X., Tan, G., Jonas, J. B., Lamoureux, E. L., Cheng, C. Y., Klein, B. E. K., Mitchell, P., Klein, R., Cheung, C. M. G., & Wong, T. Y. (2019). Incidence and progression of diabetic retinopathy: A systematic review. *The Lancet Diabetes and Endocrinology*, *7*(2), 140–149. https://doi.org/10.1016/s2213-8587(18)30128-1

Schneider, C. A., Rasband, W. S., & Eliceiri, K. W. (2012). NIH image to ImageJ: 25 years of image analysis. *Nature Methods*, *9*(7), 671–675. https://doi.org/10.1038/nmeth.2089

Sherry, E. B., Lee, P., & Choi, I.-Y. (2015). *In vivo* NMR studies of the brain with hereditary or acquired metabolic disorders. *Neurochemical Research*, *40*(12), 2647–2685. https://doi.org/10.1007/s11064-015-1772-1

Sinha, S., Ekka, M., Sharma, U. P. R., Pandey, R. M., & Jagannathan, N. R. (2014). Assessment of changes in brain metabolites in Indian patients with type-2 diabetes mellitus using proton magnetic resonance spectroscopy. *BMC Research Notes*, *7*, 41. https://doi.org/10.1186/1756-0500-7-41

Sun, H., Saeedi, P., Karuranga, S., Pinkepank, M., Ogurtsova, K., Duncan, B. B., Stein, C., Basit, A., Chan, J. C. N., Mbanya, J. C., Pavkov, M. E., Ramachandaran, A., Wild, S. H., James, S., Herman, W. H., Zhang, P., Bommer, C., Kuo, S., Boyko, E. J., & Magliano, D. J. (2022). IDF Diabetes Atlas: Global, regional and country-level diabetes prevalence estimates for 2021 and projections for 2045. *Diabetes Research and Clinical Practice*, *183*, 109119. https://doi.org/10.1016/j.diabres.2021.109119

Thielen, J. W., Gancheva, S., Hong, D., Rohani Rankouhi, S., Chen, B., Apostolopoulou, M., Anadol-Schmitz, E., Roden, M., Norris, D. G., & Tendolkar, I. (2019). Higher GABA concentration in the medial prefrontal cortex of Type 2 diabetes patients is associated with episodic memory dysfunction. *Human Brain Mapping*, *40*(14), 4287–4295. https://doi.org/10.1002/hbm.24702

Thomas, M. C., Brownlee, M., Susztak, K., Sharma, K., Jandeleit-Dahm, K. A., Zoungas, S., Rossing, P., Groop, P. H., & Cooper, M. E. (2015). Diabetic kidney disease. *Nature Reviews Disease Primers*, *1*, 15018. https://doi.org/10.1038/nrdp.2015.18

Tkác, I., Starcuk, Z., Choi, I.-Y., & Gruetter, R. (1999). *In vivo* ^{1}H NMR spectroscopy of rat brain at 1 ms echo time. *Magnetic Resonance in Medicine*, *41*(4), 649–656. https://doi.org/10.1002/(sici)1522-2594(199904)41:4<649::aid-mrm2>3.0.co;2-g

van Bussel, F. C. G., Backes, W. H., Hofman, P. A. M., Puts, N. A. J., Edden, R. A. E., van Boxtel, M. P. J., Schram, M. T., Stehouwer, C. D. A., Wildberger, J. E., & Jansen, J. F. A. (2016). Increased GABA concentrations in type 2 diabetes mellitus are related to lower cognitive functioning. *Medicine (Baltimore)*, *95*(36), e4803. https://doi.org/10.1097/md.0000000000004803

van der Graaf, M., Janssen, S. W., van Asten, J. J., Hermus, A. R., Sweep, C. G., Pikkemaat, J. A., Martens, G. J., & Heerschap, A. (2004). Metabolic profile of the hippocampus of Zucker Diabetic Fatty rats assessed by in vivo 1H magnetic resonance spectroscopy. *NMR in Biomedicine*, *17*(6), 405–410. https://doi.org/10.1002/nbm.896

Walls, A. B., Waagepetersen, H. S., Bak, L. K., Schousboe, A., & Sonnewald, U. (2015). The glutamine-glutamate/GABA cycle: Function, regional differences in glutamate and GABA production and effects of interference with GABA metabolism. *Neurochemical Research*, *40*(2), 402–409. https://doi.org/10.1007/s11064-014-1473-1

Wang, W. T., Lee, P., Yeh, H. W., Smirnova, I. V., & Choi, I.-Y. (2012). Effects of acute and chronic hyperglycemia on the neurochemical profiles in the rat brain with streptozotocin-induced diabetes detected using in vivo ^{1}H MR spectroscopy at 9.4 T. *Journal of Neurochemistry*, *121*(3), 407–417. https://doi.org/10.1111/j.1471-4159.2012.07698.x

Wang, Y., Sun, L., He, G., Gang, X., Zhao, X., Wang, G., & Ning, G. (2021). Cerebral perfusion alterations in type 2 diabetes mellitus—A systematic review. *Frontiers in Neuroendocrinology*, *62*, 100916. https://doi.org/10.1016/j.yfrne.2021.100916

Wu, G. Y., Zhang, Q., Wu, J. L., Jing, L., Tan, Y., Qiu, T. C., & Zhao, J. (2017). Changes in cerebral metabolites in type 2 diabetes mellitus: A meta-analysis of proton magnetic resonance spectroscopy. *Journal of Clinical Neuroscience*, *45*, 9–13. https://doi.org/10.1016/j.jocn.2017.07.017

Wu, P., Shi, X., Luo, M., Inam, U. L., Li, K., Zhang, M., Ma, J., Li, Y., Liu, Y., Zhang, C., Liu, X., Li, S., Li, Q., Chen, X., Che, X., & Piao, F. (2020). Taurine inhibits neuron apoptosis in hippocampus of diabetic rats and high glucose exposed HT-22 cells via the NGF-Akt/Bad pathway. *Amino Acids*, *52*(1), 87–102. https://doi.org/10.1007/s00726-019-02810-6

Yun, J. S., & Ko, S. H. (2021). Current trends in epidemiology of cardiovascular disease and cardiovascular risk management in type 2 diabetes. *Metabolism*, *123*, 154838. https://doi.org/10.1016/j.metabol.2021.154838

Zhao, X., Han, Q., Gang, X., & Wang, G. (2018). Altered brain metabolites in patients with diabetes mellitus and related complications—Evidence from ^{1}H MRS study. *Bioscience Reports*, *38*(5), BSR20180660. https://doi.org/10.1042/bsr20180660

Zheng, H., Zheng, Y., Wang, D., Cai, A., Lin, Q., Zhao, L., Chen, M., Deng, M., Ye, X., & Gao, H. (2017). Analysis of neuron-astrocyte metabolic cooperation in the brain of db/db mice with cognitive decline using 13C NMR spectroscopy. *Journal of Cerebral Blood Flow and Metabolism*, *37*(1), 332–343. https://doi.org/10.1177/0271678x15626154

Zheng, H., Zheng, Y., Zhao, L., Chen, M., Bai, G., Hu, Y., Hu, W., Yan, Z., & Gao, H. (2017). Cognitive decline in type 2 diabetic db/db mice may be associated with brain region-specific metabolic disorders. *Biochimica et Biophysica Acta—Molecular Basis of Disease*, *1863*(1), 266–273. https://doi.org/10.1016/j.bbadis.2016.11.003

Zheng, Y., Yang, Y., Dong, B., Zheng, H., Lin, X., Du, Y., Li, X., Zhao, L., & Gao, H. (2016). Metabonomic profiles delineate potential role of glutamate-glutamine cycle in *db/db* mice with diabetes-associated cognitive decline. *Molecular Brain*, *9*, 40. https://doi.org/10.1186/s13041-016-0223-5

SUPPORTING INFORMATION

Additional supporting information can be found online in the Supporting Information section at the end of this article.

How to cite this article: Choi, I.-Y., Wang, W.-T., Kim, B., Hur, J., Robbins, D. C., Jang, D.-G., Savelieff, M. G., Feldman, E. L., & Lee, P. (2024). Non-invasive in vivo measurements of metabolic alterations in the type 2 diabetic brain by ^{1}H magnetic resonance spectroscopy. *Journal of Neurochemistry*, *168*, 765–780. https://doi.org/10.1111/jnc.15996